Bioconjugate Chemistry

pubs.acs.org/bc

Article

Evaluating the Effect of Dye−Dye Interactions of Xanthene-Based Fluorophores in the Fluorosequencing of Peptides

James L. Bachman, Christopher D. Wight, Angela M. Bardo, Amber M. Johnson, Cyprian I. Pavlich, Alexander J. Boley, Holden R. Wagner, Jagannath Swaminathan, Brent L. Iverson,* Edward M. Marcotte,* and Eric V. Anslyn*

Cite This: https://doi.org/10.1021/acs.bioconjchem.2c00103

Read Online

ACCESS | Metrics & More | Article Recommendations | Supporting Information

ABSTRACT: A peptide sequencing scheme utilizing fluorescence microscopy and Edman degradation to determine the amino acid position in fluorophore-labeled peptides was recently reported, referred to as fluorosequencing. It was observed that multiple fluorophores covalently linked to a peptide scaffold resulted in a decrease in the anticipated fluorescence output and worsened the single-molecule fluorescence analysis. In this study, we report an improvement in the photophysical properties of fluorophore-labeled peptides by incorporating long and flexible $(PEG)_{10}$ linkers at the peptide attachment points. Long linkers to the fluorophores were installed using copper-catalyzed azide−alkyne cycloaddition conditions. The photophysical properties of these peptides were analyzed in solution and immobilized on a microscope slide at the single-molecule level under peptide fluorosequencing conditions. Solution-phase fluorescence analysis showed improvements in both quantum yield and fluorescence lifetime with the long linkers. While on the solid support, photometry measurements showed significant increases in fluorescence brightness and 20 to 60% improvements in the ability to determine the amino acid position with fluorosequencing. This spatial distancing strategy demonstrates improvements in the peptide sequencing platform and provides a general approach for improving the photophysical properties in fluorophore-labeled macromolecules.

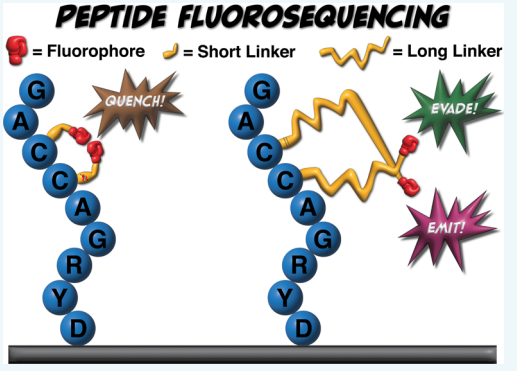

INTRODUCTION

Fluorescence imaging has been integral to the development of several impactful technologies, especially in the chemical biology toolset, including activity-based probes[1−11] and methods for visualizing cellular structures.[12−21] Small-molecule fluorophores are uniquely enabling in analytical applications due to their size, ease of use, and modularity.[22,23] In combination with single-molecule fluorescence microscopy techniques, these probes have shed light on a number of challenging biological problems.[24−27] One of the most widely used families of fluorescent probes are based on the xanthene scaffold. Ever since their initial discovery in the late 19th century, the xanthene fluorophores, fluorescein (**1**) and rhodamine (**2**), have found abundant use (Figure 1A).[28] The parent compounds themselves are highly modifiable at the xanthene core and through substituents at the pendant aryl group or aniline. In the case of rhodamine, variants have also been prepared by substituting the central oxygen atom to give fluorophores such as the carbopyronine Atto 647N (**3**),[29−32] among others.[33−37] Xanthene-based dyes generally possess desirable spectral properties, including high extinction coefficients and quantum yields (QYs), fluorescence in the visible region, and overall chemical stability.[38] However, a key drawback to these fluorescent probes is their tendency for fluorescence self-quenching.

The self-quenching of **1** is a well-documented observation in the fluorescence microscopy analysis of fluorescein-labeled biomolecules[39−41] and has also been shown to occur with rhodamine fluorophores.[42−45] Increasing the number of fluorophores on a scaffold gives rise to a nonlinear increase in fluorescence intensity and a shortened fluorescent lifetime (FLT),[46,47] and in extreme cases, actually leads to inhibition of fluorescence.[48] The fluorescence self-quenching of fluorescein has been attributed to interactions through a fluorescence resonance-energy transfer (FRET) mechanism.[49,50] In contrast, rhodamines not only demonstrate dramatic fluorescence quenching primarily by dimerization through J- and H-aggregates depending upon the solvent but can also engage in FRET. Comparatively, carbopyronines such as **3** remain

Received: February 28, 2022
Revised: April 13, 2022

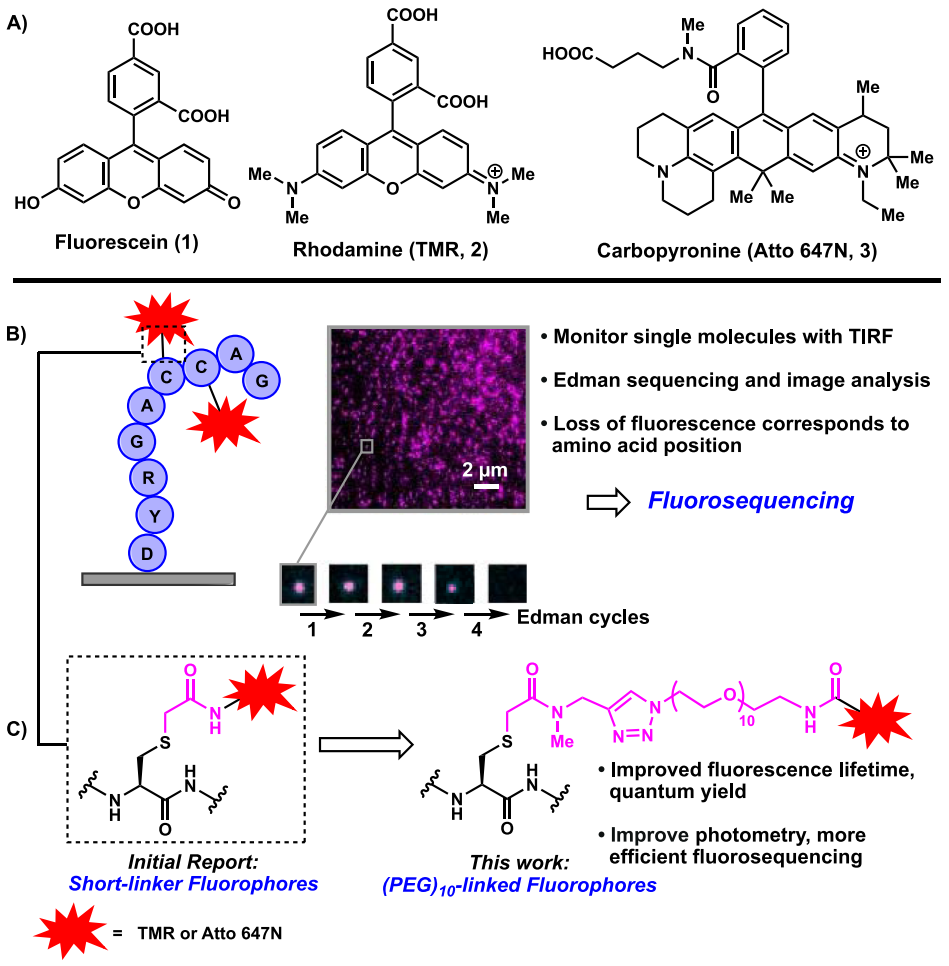

Figure 1. Common xanthene fluorophores and overview of peptide fluorosequencing. (A) Structures of xanthene fluorophores and the two fluorophores used in the initial fluorosequencing report (2 and 3). (B) Bis-cysteine peptide with fluorophores at positions 3 and 4 being monitored with single-molecule fluorescence microscopy. A single fluorescent spot is representative of the di-labeled peptide, with corresponding loss of fluorescence for that spot occurring during the third and fourth Edman degradation cycles. (C) Initial report had short linkers between the fluorophores and the peptide backbone. The longer PEG_{10} linker shown is discussed herein.

underexplored in this regard.[51−53] These two quenching mechanisms can operate in systems where multiple fluorescent probes of the same identity are covalently linked to scaffolds such as peptides[54] and thus can complicate analyses that rely upon reading the fluorescence output.

These challenges were highlighted in a recent report by our group that detailed a strategy for identifying the amino acid sequence of short peptides by analyzing the fluorescence of xanthene fluorophores covalently attached to amino acid side chains in a scheme known as "fluorosequencing" (Figure 1B).[55] Notably, fluorosequencing is just one of many emerging techniques in the field of single-molecule protein sequencing.[56] While the next-generation techniques in the area of genomic sequencing have revolutionized diagnostics, the analogous technique for proteins is still lacking. In the fluorosequencing approach, fluorophore-labeled peptides are covalently attached to a solid support via the *C*-terminus, where fluorescence is analyzed using total internal reflection fluorescence (TIRF) microscopy at single-molecule resolution.[57] During analysis, peptides are subjected to Edman degradation chemistry, which removes the *N*-terminal amino acid in each Edman cycle.[58] Thus, when a nonlabeled amino acid is cleaved, no change in the fluorescence output is observed, but when a fluorophore-labeled amino acid is cleaved, the fluorescence signal for that residue is lost, which indicates the identity of the amino acid residue.[59]

While a broad range of fluorophores were evaluated for this sequencing strategy, given the harsh conditions of Edman degradation,[60] we found that only xanthene-based dyes tetramethyl rhodamine (**2**) and carbopyronine Atto 647N (**3**) possessed the desired survivability and photophysical properties required for fluorosequencing (Figure 1A).[61] However, as expected, peptides labeled with multiple fluorophores of the same identity were more challenging to sequence.[62] Notably, the difficulty in sequencing was accentuated when the fluorophores were spatially close on the peptide backbone. As a result, we sought a strategy for minimizing the quenching interactions between appended fluorophores. The two avenues we considered to apply were the use of metals to enhance fluorescence, as demonstrated by a number of groups,[63−66] or to alter the length of the fluorophore linker, a surprisingly understudied area.[67] For the experimental setup, it was anticipated that metal additives could complicate analysis and potentially be degraded under Edman conditions. Thus, despite the considerable additional synthetic effort required to incorporate, we developed a methodology for attaching fluorophores **2** and **3** that possessed long, flexible linkers to cysteine residues using copper-catalyzed

https://doi.org/10.1021/acs.bioconjchem.2c00103
Bioconjugate Chem. XXXX, XXX, XXX−XXX

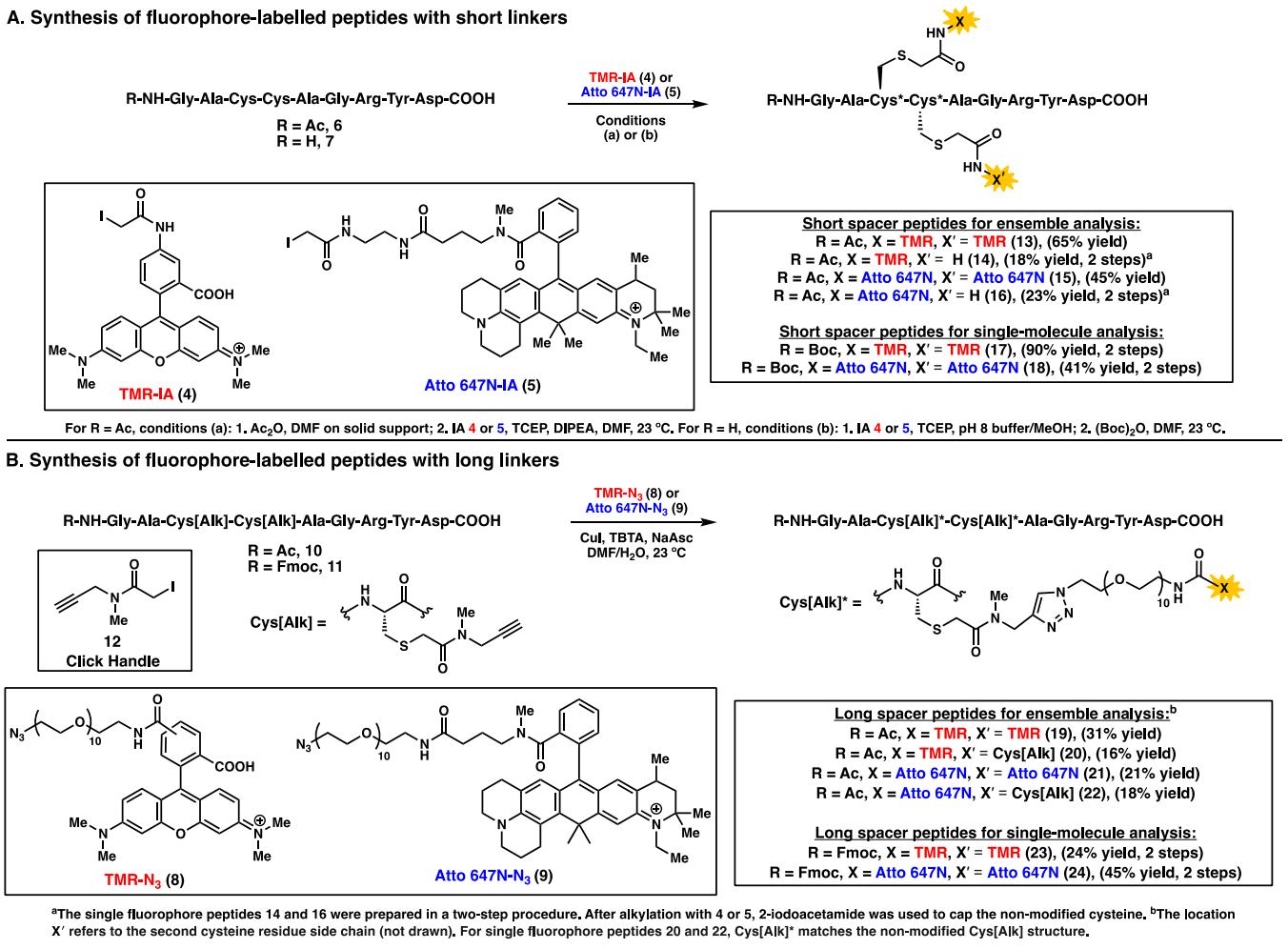

Figure 2. Design and synthesis of short- and long-linker peptides used to study photophysical and peptide fluorosequencing properties.

click chemistry. This report will detail our approach, synthetic efforts, and fluorescence analysis of peptides labeled with fluorophores using $(PEG)_{10}$ linkers. While unclear at the outset, it was hoped that this strategy would lead to a reduction in fluorescence quenching by minimizing the ability of fluorophores on a peptide scaffold to interact and thus improve the efficiency of peptide fluorosequencing.

In our initial report, peptides were prepared by modifying the cysteine residues with iodoacetamide derivatives of TMR (**4**) and Atto 647N (**5**) (Figure 2A). This conjugation handle is selective for labeling cysteine residues,[68] and these derivatives are commercially available. The iodoacetamide handle is tethered to the fluorophores by linkers that are relatively short, as in **4** and **5**, albeit the linker in **5** is longer than that in **4**. Thus, when peptides, such as GACCAGRYD (**7**) are labeled with fluorophores at the third and fourth residues, the fluorophores are in quite close proximity and can engage in interactions such as aggregation that leads to fluorescence quenching.

For the current study, parent peptide **7** was selected to test our fluorophore spacing postulate. Based on our prior work,[55] we found peptides with fluorophores at adjacent positions particularly challenging to sequence. As such, we chose to place the cysteine residues next to one another in an effort to maximize the interaction, anticipating that the longer linker would decrease interactions and thus lead to a greater improvement in amino acid identification. Labeling at the third and fourth positions meant that the fluorophores would only need to undergo four rounds of Edman degradation to sequence the peptides, lowering overall experimental run time.[69] Additionally, the nine-residue oligopeptide was large enough to enable simple synthesis by solid-phase peptide synthesis (SPPS) and chemical manipulation. As our initial report was intended to demonstrate the sequencing of model peptides that could be derived from real human proteins, the sequence was intentionally made less than 20 amino acids and terminated in an aspartic acid residue to mimic protein digestion by Endoproteinase GluC. In particular, peptides were synthesized and covalently bound to fluorophores through both short-linker units (as shown in **4** and **5**) and longer $(PEG)_{10}$ linkers (as shown in **8** and **9**) (Figure 2). While the short-linker fluorophores could be incorporated through standard cysteine alkylation, the long-linker fluorophores were installed onto the alkyne-modified peptide **11** using copper-catalyzed azide−alkyne cycloaddition (CuAAC) conditions. Peptide **11** was accessed from Fmoc-protected variant of peptide **7** by alkylation with click handle **12**.[70] The specific $(PEG)_{10}$ spacers were chosen due to commercial availability of the linker as a hetero-functionalized polyethylene glycol unit.[71] The free amine of the linker allowed for simple incorporation into the fluorophores through amide coupling, while the azide functional group allowed for the click installation to the peptides.[72] To evaluate the photophysical differences between the short-linker fluorophore-labeled peptides and the long-

https://doi.org/10.1021/acs.bioconjchem.2c00103
Bioconjugate Chem. XXXX, XXX, XXX−XXX

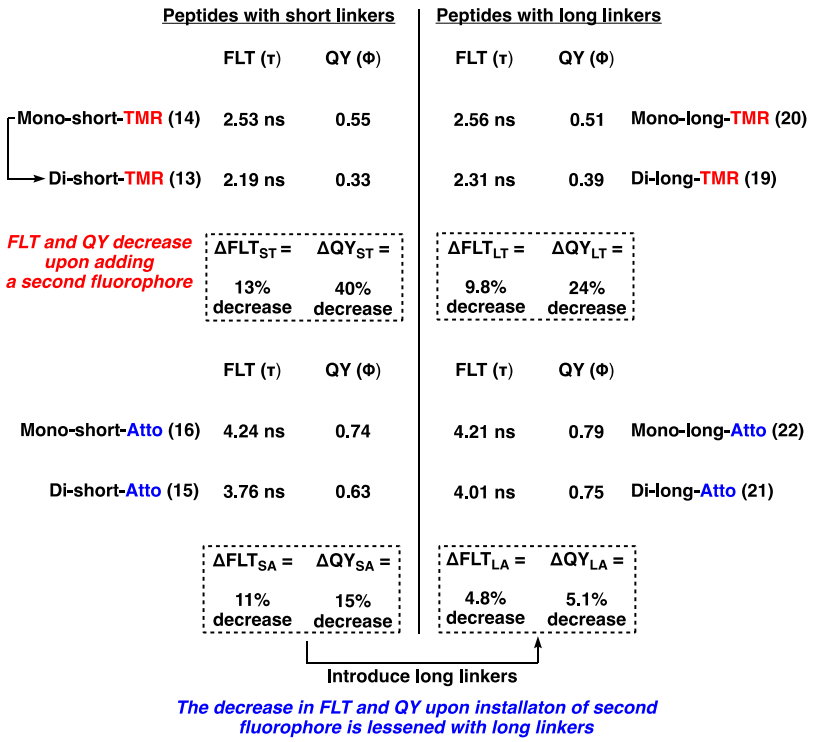

Figure 3. Solution-phase analysis of peptide QY (Φ) and FLT (τ, ns). Nomenclature for fluorophore-labeled peptides: ST = short-linker, TMR; LT = long-linker, TMR; SA = short-linker, Atto 647N; and LA = long-linker, Atto 647N.

linker peptides, we performed both solution-phase and single-molecule fluorescence analyses.

Peptides for bulk fluorescence analysis, which included FLT and QY measurements, were acetylated at the *N*-terminus.[73] Short-linker peptides for this purpose were **13**−**16**, and long-linker peptides were **19**−**22**. Within these sets of peptides, both single fluorophore-labeled and di-labeled peptides were prepared. The single fluorophore peptides represent the baseline for the photophysical properties that could be compared to the di-labeled peptides, where it was expected that the fluorescence output would be modified by the introduction of the second fluorophore onto the peptide scaffold. The differences in FLT and QY between these sets of peptides then allowed quantification of linker length effects on ensemble photophysics.

Separately, another group of peptides were synthesized that possessed removable *N*-terminal protecting groups (Boc or Fmoc) for use in the single-molecule fluorosequencing routine: **17**, **18**, **23**, and **24**. For these peptides, the removable protecting group was necessary to allow for solid-support attachment followed by Edman degradation to carry out fluorosequencing.

PEPTIDE SYNTHESIS

As shown in Figure 2, a total of 12 peptides were prepared for this study, each of which was used in the manner presented above. The short-linker peptides used in ensemble analysis, **13**, **14**, **15**, and **16**, were prepared from acetylated peptide **6** using reaction conditions (a) (Figure 2A). Fluorophores were installed by alkylation under anhydrous conditions with the corresponding fluorophore-iodoacetamide derivative (**4** or **5**). Notably, single fluorophore peptides **14** and **16** were prepared in a two-step procedure by first alkylating with 1 equivalent of fluorophore followed by the corresponding 2-iodoacetamide (giving inseparable mixtures of position 3 and 4 labeling).[74] Short-linker peptides for fluorosequencing analysis were prepared with a Boc protecting group on the *N*-terminus. Using reaction conditions (b) (Figure 2A), alkylation of peptide **7** with fluorophore **4** or **5** in aqueous buffer followed by subjection to Boc anhydride under anhydrous conditions gave peptides **17** and **18**, respectively.

The long-linker peptides for this study were prepared from alkyne-functionalized peptides **10** and **11** (Figure 2B), which were accessed by alkylation of **6** or a variant of **6** (R = Fmoc, **28**, see SI) with iodoacetamide click handle **12**. The fluorophore-labeled peptides for ensemble analysis, **19**, **20**, **21**, and **22**, were prepared by subjecting peptide **10** to copper-catalyzed conditions using TBTA (Tris[(1-benzyl-1*H*-1,2,3-triazol-4-yl)methyl]amine) as a ligand with azide-fluorophores **8** or **9**. As with the short-linker peptides, two peptides labeled with a single fluorophore and one nonfluorescent handle on the second cysteine residue were prepared, **20** and **22**. The peptides for fluorosequencing were prepared from Fmoc-protected peptide **11**,[75] which was incorporated from the SPPS. Again, subjecting **11** to the same copper-catalyzed click conditions with **8** or **9** gave access to peptides **23** and **24**, respectively. Overall, long-linker peptide preparation generally proceeded by way of lower yield than the corresponding short-linker peptides, likely due to the challenge of CuAAC occurring between such large subunits (1 KDa each). However, due to the very low concentrations required for both solution phase and single-molecule analyses, even low yielding reactions on sub milligram quantities enabled this study.

ENSEMBLE FLUORESCENCE ANALYSIS

With the peptides synthesized, we first characterized the ensemble fluorescent properties. Using short-linker peptides

https://doi.org/10.1021/acs.bioconjchem.2c00103
Bioconjugate Chem. XXXX, XXX, XXX−XXX

13−**16** and long-linker peptides **19**−**22**, we sought to evaluate trends in the FLT (τ) and QY (Φ) between the two sets of peptides. This analysis would allow us to glean insights into the possible quenching pathways occurring in these peptides. Aggregation-induced fluorescence quenching occurs via a static mechanism, where the two or more fluorophores form a nonfluorescent species, decreasing fluorescence intensity and QY but minorly altering FLT.[46,47] In contrast, FRET-based quenching is a dynamic, through-space mechanism, where a decrease in FLT is generally observed.[50,51] The single fluorophore-labeled peptides represent the baseline of photophysical properties, with the di-labeled peptides representing an increase in the relative fluorophore concentration. The observed changes in QY and FLT upon an increase in fluorophore concentration can then give insight into the dye−dye interactions that are occurring.

The experimentally determined QY and FLTs[76] of peptides **13**−**16** and **19**−**22** are reported in Figure 3. To begin the analysis, starting from the mono-short-TMR peptide **14**, the introduction of a second fluorophore, as in di-short-TMR peptide **13**, resulted in a decrease in both the FLT and QY. The differences between the mono-fluorophore values and the di-fluorophore values for the short-linker TMR peptides are ΔFLT_{ST} and ΔQY_{ST} (ST = short-linker, TMR). To evaluate the improvement in photophysical properties seen by using the $(PEG)_{10}$ linkers, the values of ΔFLT_{ST} and ΔQY_{ST} are compared to the same values determined for the long-linker peptides of the same fluorophore (e.g., ΔFLT_{LT} and ΔQY_{LT}). In this way, the effect of long-linker tethers on the QY and FLT could be quantified.

The mono-short-TMR peptide **14** was found to have a FLT of 2.53 ns and a QY of 0.55. Upon the installation of a second TMR fluorophore as in di-short-TMR (**13**), a FLT of 2.19 ns and a QY 0.33 were observed. The introduction of the second fluorophore resulted in FLT decrease of 13% (ΔFLT_{ST}) and a QY decrease of 40% (ΔQY_{ST}). The same calculations were performed for the long-linker TMR peptides **19** and **20**, to determine the effect of the linker change. For the mono-long-TMR peptide **20**, a FLT of 2.56 ns and a QY of 0.51 were found. Upon installation of a second TMR fluorophore, as in di-long-TMR (**19**), a FLT of 2.31 ns and a QY of 0.39 were observed. In this case, introducing the second fluorophore led to a FLT decrease of 9.8% (ΔFLT_{LT}) and a QY decrease of 24% (ΔQY_{LT}).

For TMR-labeled peptides, a 13% decrease in FLT with the short-linker peptides (ΔFLT_{ST}) was found, compared to a 9.8% decrease in FLT with the long-linker peptides (ΔFLT_{LT}). The longer linkers resulted in an improvement in fluorescence lifetime by a factor of 1.3. More pronounced, however, is the improvement in the QY. The QY decrease for the short-linker-TMR peptides of 40% (ΔQY_{ST}) compared to the 24% QY decrease for the long-linker peptides (ΔQY_{LT}) represents an improvement in the QY of the peptide−fluorophore conjugate by a factor of 1.7. Taken together, for TMR peptides, the improvements in both FLT and QY using the long-linker strategy validate our hypothesis that increasing the spacing and flexibility of peptide attachment points would improve the photophysical properties of the appended fluorophores.

The same analysis was performed for the Atto 647N-labeled peptides. The mono-short-Atto peptide **16** was found to have a FLT of 4.24 ns and a QY of 0.74. Comparatively, the di-short-Atto (**15**) had a FLT of 3.76 ns and a QY of 0.63. Taken together, for short-linker Atto 647N peptides, a decrease in FLT of 11% (ΔFLT_{SA}) and a QY decrease of 15% (ΔQY_{SA}) were observed when a second Atto 647N fluorophore was introduced to the peptide. The same calculations were then performed for the long-linker Atto 647N peptides. Mono-long-Atto peptide **22** had a FLT of 4.21 ns and a QY of 0.79 compared to di-long-Atto (**21**), which had a FLT of 4.01 ns and a QY of 0.75. Thus, for long-linker Atto 647N peptides, a FLT decrease of 4.8% (ΔFLT_{LA}) and a QY decrease of 5.1% (ΔQY_{LA}) were observed upon the introduction of the second fluorophore onto the peptide.

For short-linker Atto 647N-labeled peptides, the FLT decrease of 11% (ΔFLT_{SA}) compared to the 4.8% decrease for the long-linker peptides (ΔFLT_{LA}) shows an improvement in fluorescence lifetime by a factor of 2.3 using long $(PEG)_{10}$ linkers. Similarly, the decrease in QY for the short-linker peptides of 15% (ΔQY_{SA}) as compared to 5.1% in the long-linker peptides (ΔQY_{LA}) shows an improvement in the QY by a factor of 2.9. With these results, we reach a similar conclusion to the TMR-labeled peptides: the smaller decreases in fluorescence lifetime and QY reflect a decrease in fluorescence quenching and thus an improvement in photophysical properties.

In the TMR-labeled peptides, the relatively small improvements in FLT (1.3-fold) and QY (1.7-fold) found when using long-linkers can likely be rationalized by considering a fluorescence quenching mechanism that proceeds primarily by dimerization. It has been widely reported that rhodamine fluorophores engage in aggregation-induced quenching,[51,53] and this is the most likely interaction occurring in peptides **13** and **19**. With the $(PEG)_{10}$ linker strategy, the long distance installed between the fluorophores can perturb the dimerization pathways, perhaps minimizing it or slowing the rate of dimerization due to the added degrees of freedom but not inhibiting it altogether. As such, improvements are observed in the photophysical properties, albeit modest ones. For the Atto 647N-labeled peptides, significantly larger improvements in both FLT (2.3-fold) and QY (2.9-fold) were observed when using the long-linker strategy. These larger changes observed in the $(PEG)_{10}$ linker molecules could be due to either disruption of a homo-FRET-type quenching mechanism or the same dimerization inhibition as with TMR. To the best of our knowledge, this is an understudied area of research with respect to carbopyronine fluorophores.

SINGLE-MOLECULE FLUOROSEQUENCING ANALYSIS

As a companion to the ensemble fluorescence analysis, we also employed single-molecule fluorescence microscopy to evaluate the effect of linker length on peptide fluorosequencing efficiencies. The purpose of fluorosequencing is to identify the position of the fluorophore-labeled amino acid residues within a peptide sequence, giving a partial sequence. In modeling, our group has previously demonstrated that proteins in complex mixtures can be identified from the information contained in partial peptide sequences.[77] Fluorosequencing, like other single-molecule-based methods, enables decoupling of dynamic signal variance caused within a molecule from environmental variances observed between molecules.[78] Additionally, the fluorosequencing method enables the analysis of the same peptide before and after the removal of a fluorophore-labeled amino acid.

To this end, peptides **17**, **18**, **23**, and **24** were subjected to single-molecule fluorosequencing, as described by us in detail

https://doi.org/10.1021/acs.bioconjchem.2c00103
Bioconjugate Chem. XXXX, XXX, XXX−XXX

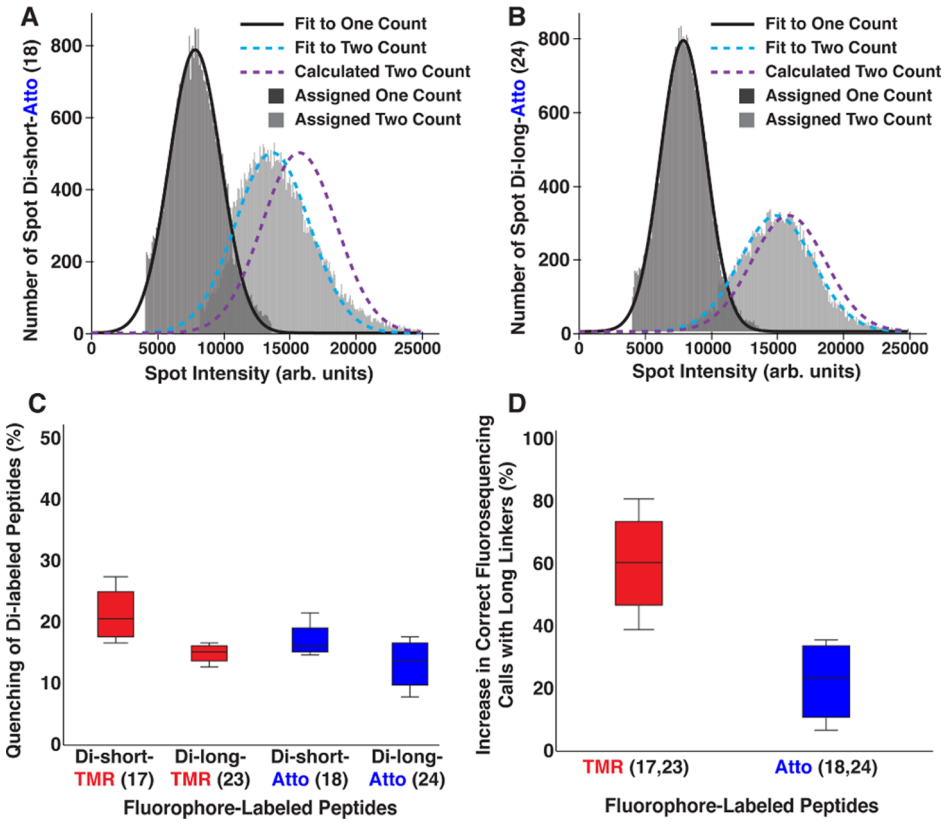

Figure 4. Intensity distribution and Gaussian fits for (A) short-linker Atto (**18**) and (B) long-linker Atto (**24**). (C) Percent quenching of peptides **17**, **18**, **23**, and **24**, showing a clear decrease in quenching with long linkers. (D) Percent change in correct positional assignments in fluorosequencing from short to long linkers for TMR (**17** to **23**) and Atto 647N (**18** to **24**).

previously.[55] This particular analysis provides a fluorophore count assignment for each peptide after each round of Edman degradation, which is used to determine the position of the labeled amino acids. For peptides of parent sequence GACCAGRYD, the expected fluorophore count assignments after five rounds of Edman degradation would be 2, 2, 1, 0, 0 with a drop from 2 to 1 after the third Edman cycle and 1 to 0 at the fourth Edman cycle, representing the loss of the fluorophore-labeled cysteines (see Figure 1B). Four unique fluorosequencing analyses were performed for each peptide **17**, **18**, **23**, and **24**.

To evaluate quenching in these peptides, the count assignments from each sequencing experiment were collected for every Edman degradation cycle and then sorted by their fluorophore count based on photometry analysis. The number of one- and two-count assignments (i.e., loss of only one fluorophore and expected loss of two fluorophores, respectively) were plotted as separate histograms and fit with a Gaussian distribution to determine the mean spot intensity for short- (**17**, **18**) and long-linker peptides (**23**, **24**).[79] Representative examples of these histograms and fits are shown in Figure 4A for the di-labeled short-linker Atto 647N peptide **18** and in Figure 4B for the di-labeled long-linker Atto 647N peptide **24**, where the fits for one-count assignments are shown as a black solid line and the fits for two-count assignments are shown as a dashed teal line. The effects of self-quenching can be visualized by first plotting the expected distribution of the calculated unquenched two-count signal as a doubling of the mean of the single-count distribution, represented on Figure 4A,B as a dashed purple line. Second, we compare the two-count signal (teal line) to this doubling of the mean for a one-count peptide. We find that the dotted lines better overlay with the longer linkers; in other words, the experimental distribution for the peptides with two counts (Figure 4B) fits the calculated distribution better than that with the shorter-linker tethers (Figure 4A). Hence, the $(PEG)_{10}$-linked attachment indeed improves the fluorosequencing results.

To quantify this improvement, the fluorescence quenching was calculated as the percent difference between the calculated, unquenched, two-fluorophore signal mean and the mean of the experimentally collected two-fluorophore signal distribution. The resultant values are plotted in Figure 4C and show a significant decrease in quenching from the short-linker peptides to long-linker peptides with TMR [from 22 ± 2% (**17**) to 16 ± 3% (**23**)]. A similar effect, albeit smaller, occurs with the Atto 647N-labeled peptides, where the fluorescence quenching drops from 17 ± 1% (**18**) to 15 ± 3% (**24**).

Lastly, the sequencing assignments were used to evaluate the degree to which the length of the linkers affects the correct positional assignments in the fluorosequencing analysis. Figure 4D shows the percent increase in correct assignments for long-linker peptides versus short-linker peptides. Here, the TMR case showed a dramatic effect, with a 60% improvement in sequencing long-linker peptide **23** compared to short-linker peptide **17**. Again, for peptides labeled with Atto 647N, the change was less pronounced but still quite significant; a 23% improvement when sequencing long-linker peptide **24** compared to short-linker peptide **18**. These results demonstrate that the strategy of spatially distancing fluorophores on a

https://doi.org/10.1021/acs.bioconjchem.2c00103
Bioconjugate Chem. XXXX, XXX, XXX−XXX

peptide backbone led to improvements in the photophysical properties of the peptide−fluorophore conjugates and ease of application.

CONCLUSIONS

Single-molecule techniques for the sequencing of biopolymers offer significant advantages for genomic and proteomic studies. For peptides, our method, referred to as fluorosequencing, uses iterative Edman degradation steps to remove fluorophore-labeled amino acid side chains, as monitored by TIRF microscopy. To improve the positional assignments of amino acids when proximal to one another by minimizing the static and dynamic quenching, we explored a strategy of increasing the spacing of the fluorophores from the peptide backbone by using longer linkers than those used in our first report. Using two different fluorophores, TMR and Atto-647N, the increased linker length (embodied by a PEG_{10}) led to significant improvements in both QYs and FLTs (factors of 1.3 to 2.9). More important, however, the improvements found in the correct positional assignments for fluorosequencing were significant. When adjacent, the correct assignments for two cysteine residues using TMR and Atto fluorophores improved by 60% and 23%, respectively. Thus, increasing the length and flexibility of the linkers between amino acid side chains and their corresponding fluorophores decreases quenching, thereby increasing QYs and FLTs, and importantly the ability to correctly sequence labeled amino acids when positioned proximally in a peptide. This advance will become a general strategy to incorporate into our fluorosequencing routines and may inform more general fluorophore attachment strategies in various scaffolds. Similarly, the use of long and flexible linkers could benefit other quantitative single-molecule applications that involve counting applications.[80,81] Although this study focuses on adjacent labels, other quenching processes could similarly benefit from increased freedom of motion and the resulting physical separation.

ASSOCIATED CONTENT

Supporting Information

The Supporting Information is available free of charge at https://pubs.acs.org/doi/10.1021/acs.bioconjchem.2c00103.

Detailed experimental data, compound characterization data, and other information (PDF)

AUTHOR INFORMATION

Corresponding Authors

Brent L. Iverson − *Department of Chemistry, The University of Texas at Austin, Austin, Texas 78712, United States;* orcid.org/0000-0001-7974-3605; Email: iversonb@austin.utexas.edu

Edward M. Marcotte − *Department of Molecular Biosciences, The University of Texas at Austin, Austin, Texas 78712, United States*; Email: Marcotte@utexas.edu

Eric V. Anslyn − *Department of Chemistry, The University of Texas at Austin, Austin, Texas 78712, United States;* orcid.org/0000-0002-5137-8797; Email: Anslyn@austin.utexas.edu

Authors

James L. Bachman − *Department of Chemistry, The University of Texas at Austin, Austin, Texas 78712, United States*

Christopher D. Wight − *Department of Chemistry, The University of Texas at Austin, Austin, Texas 78712, United States;* orcid.org/0000-0003-3389-1762

Angela M. Bardo − *Department of Molecular Biosciences, The University of Texas at Austin, Austin, Texas 78712, United States*

Amber M. Johnson − *Department of Chemistry, The University of Texas at Austin, Austin, Texas 78712, United States*

Cyprian I. Pavlich − *Department of Chemistry, The University of Texas at Austin, Austin, Texas 78712, United States*

Alexander J. Boley − *Department of Chemistry, The University of Texas at Austin, Austin, Texas 78712, United States*

Holden R. Wagner − *Department of Chemistry, The University of Texas at Austin, Austin, Texas 78712, United States*

Jagannath Swaminathan − *Department of Molecular Biosciences, The University of Texas at Austin, Austin, Texas 78712, United States*

Complete contact information is available at: https://pubs.acs.org/10.1021/acs.bioconjchem.2c00103

Author Contributions

J.L.B. and C.D.W. contributed equally. J.L.B., A.M.B., A.M.J., J.S., E.M.M., and E.V.A. conceptualized the project. J.L.B., C.D.W., and A.M.B. designed and supervised experiments. J.L.B., C.D.W., A.M.J., C.I.P, and A.J.B. synthesized and characterized the compounds. C.D.W. and H.R.W conducted solution phase fluorescence characterization and analysis. J.L.B. and A.M.B. conducted single-molecule fluorescence microscopy experiments and analysis. E.V.A., E.M.M., and B.L.I. provided funding for the project. The manuscript was written by J.L.B, C.D.W., A.M.B., and E.V.A, with editing and review from all authors.

Notes

The authors declare the following competing financial interest(s): J.S., E.M.M., A.B. and E.V.A. are co-founders and shareholders of Erisyon, Inc.

ACKNOWLEDGMENTS

This work was supported by grants from DARPA (N66001-14-2-4051 to E.V.A. and E.M.M.), NIH (R35 GM122480, R01 HD085901, and R01 DK110520 to E.M.M.), Erisyon, Inc. (to E.M.M. and E.V.A.), and the Welch foundation (F-1515 to E.M.M. and F-1188 to B.L.I.), and the Welch Regents Chair (F-0046) to E.VA. J.S., E.M.M., A.J.B., and E.V.A. are co-founders and shareholders of Erisyon, Inc.

REFERENCES

(1) Heal, W. P.; Dang, T. H. T.; Tate, E. W. Activity-Based Probes: Discovering New Biology and New Drug Targets. *Chem. Soc. Rev.* **2011**, *40*, 246−257.

(2) Eun Jun, M.; Roy, B.; Han Ahn, K. "Turn-on" Fluorescent Sensing With "Reactive" Probes. *Chem. Commun.* **2011**, *47*, 7583−7601.

(3) Bruemmer, K. J.; Crossley, S. W. M.; Chang, C. J. Activity-Based Sensing: A Synthetic Methods Approach for Selective Molecular Imaging and Beyond. *Angew. Chem., Int. Ed.* **2020**, *59*, 13734−13762.

(4) Chan, J.; Dodani, S. C.; Chang, C. J. Reaction-Based Small-Molecule Fluorescent Probes for Chemoselective Bioimaging. *Nat. Chem.* **2012**, *4*, 973−984.

(5) Jun, J. V.; Chenoweth, D. M.; Petersson, E. J. Rational Design of Small Molecule Fluorescent Probes for Biological Applications. *Org. Biomol. Chem.* **2020**, *18*, 5747−5763.
(6) de Bruin, G.; Xin, B. T.; Kraus, M.; van der Stelt, M.; van der Marel, G. A.; Kisselev, A. F.; Driessen, C.; Florea, B. I.; Overkleeft, H. S. A Set of Activity-Based Probes to Visualize Human (Immuno)-proteasome Activities. *Angew. Chem., Int. Ed.* **2016**, *55*, 4199−4203.
(7) Bruemmer, K. J.; Walvoord, R. R.; Brewer, T. F.; Burgos-Barragan, G.; Wit, N.; Pontel, L. B.; Patel, K. J.; Chang, C. J. Development of a General Aza-Cope Reaction Trigger Applied to Fluorescence Imaging of Formaldehyde in Living Cells. *J. Am. Chem. Soc.* **2017**, *139*, 5338−5350.
(8) Lin, V. S.; Chen, W.; Xian, M.; Chang, C. J. Chemical Probes for Molecular Imaging and Detection of Hydrogen Sulfide and Reactive Sulfur Species in Biological Systems. *Chem. Soc. Rev.* **2015**, *44*, 4596−4618.
(9) Lim, M. H.; Xu, D.; Lippard, S. J. Visualization of Nitric Oxide in Living Cells by a Copper-Based Fluorescent Probe. *Nat. Chem. Biol.* **2006**, *2*, 375−380.
(10) Chang, M. C. Y.; Pralle, A.; Isacoff, E. Y.; Chang, C. J. A Selective, Cell-Permeable Optical Probe for Hydrogen Peroxide in Living Cells. *J. Am. Chem. Soc.* **2004**, *126*, 15392−15393.
(11) Xia, H.-C.; Xu, X.-H.; Song, Q.-H. BODIPY-Based Fluorescent Sensor for the Recognization of Phosgene in Solutions and in Gas Phase. *Anal. Chem.* **2017**, *89*, 4192−4197.
(12) Lavis, L. D.; Raines, R. T. Bright Ideas for Chemical Biology. *ACS Chem. Biol.* **2008**, *3*, 142−155.
(13) Sletten, E. M.; Bertozzi, C. R. Bioorthogonal Chemistry: Fishing for Selectivity in a Sea of Functionality. *Angew. Chem., Int. Ed.* **2009**, *48*, 6974−6998.
(14) Shieh, P.; Bertozzi, C. R. Design Strategies for Bioorthogonal Smart Probes. *Org. Biomol. Chem.* **2014**, *12*, 9307−9320.
(15) Cañeque, T.; Müller, S.; Rodriguez, R. Visualizing Biologically Active Small Molecules in Cells Using Click Chemistry. *Nat. Rev. Chem.* **2018**, *2*, 202−215.
(16) Chyan, W.; Raines, R. T. Enzyme-Activated Fluorogenic Probes for Live-Cell and in Vivo Imaging. *ACS Chem. Biol.* **2018**, *13*, 1810−1823.
(17) Li, J.; Kong, H.; Zhu, C.; Zhang, Y. Photo-Controllable Bioorthogonal Chemistry for Spatiotemporal Control of Bio-Targets in Living Systems. *Chem. Sci.* **2020**, *11*, 3390−3396.
(18) Peng, T.; Hang, H. C. Site-Specific Bioorthogonal Labeling for Fluorescence Imaging of Intracellular Proteins in Living Cells. *J. Am. Chem. Soc.* **2016**, *138*, 14423−14433.
(19) Shieh, P.; Dien, V. T.; Beahm, B. J.; Castellano, J. M.; Wyss-Coray, T.; Bertozzi, C. R. CalFluors: A Universal Motif for Fluorogenic Azide Probes across the Visible Spectrum. *J. Am. Chem. Soc.* **2015**, *137*, 7145−7151.
(20) Dou, Y.; Wang, Y.; Duan, Y.; Liu, B.; Hu, Q.; Shen, W.; Sun, H.; Zhu, Q. Color-Tunable Light-up Bioorthogonal Probes for In Vivo Two-Photon Fluorescence Imaging. *Chem.—Eur. J.* **2020**, *26*, 4576−4582.
(21) Lee, Y.; Cho, W.; Sung, J.; Kim, E.; Park, S. B. Monochromophoric Design Strategy for Tetrazine-Based Colorful Bioorthogonal Probes with a Single Fluorescent Core Skeleton. *J. Am. Chem. Soc.* **2018**, *140*, 974−983.
(22) Gonçalves, M. S. T. Fluorescent Labeling of Biomolecules with Organic Probes. *Chem. Rev.* **2009**, *109*, 190−212.
(23) Terai, T.; Nagano, T. Small-Molecule Fluorophores and Fluorescent Probes for Bioimaging. *Eur. J. Physiol.* **2013**, *465*, 347−359.
(24) Chen, J. S.; Dagdas, Y. S.; Kleinstiver, B. P.; Welch, M. M.; Sousa, A. A.; Harrington, L. B.; Sternberg, S. H.; Joung, J. K.; Yildiz, A.; Doudna, J. A. Enhanced Proofreading Governs CRISPR−Cas9 Targeting Accuracy. *Nature* **2017**, *550*, 407−410.
(25) Singh, D.; Wang, Y.; Mallon, J.; Yang, O.; Fei, J.; Poddar, A.; Ceylan, D.; Bailey, S.; Ha, T. Mechanisms of Improved Specificity of Engineered Cas9s Revealed by Single-Molecule FRET Analysis. *Nat. Struct. Mol. Biol.* **2018**, *25*, 347−354.
(26) Lu, H. P.; Xun, L.; Xie, X. S. Single-Molecule Enzymatic Dynamics. *Science* **1998**, *282*, 1877−1882.
(27) Leake, M. C.; Chandler, J. H.; Wadhams, G. H.; Bai, F.; Berry, R. M.; Armitage, J. P. Stoichiometry and Turnover in Single, Functioning Membrane Protein Complexes. *Nature* **2006**, *443*, 355−358.
(28) Lavis, L. D. Teaching Old Dyes New Tricks: Biological Probes Built from Fluoresceins and Rhodamines. *Annu. Rev. Biochem.* **2017**, *86*, 825−843.
(29) Drexhage, K.-H.; Arden-Jacob, J.; Frantzeskos, J.; Zilles, A. Carbopyronine Fluorescent Dyes. U.S. Patent 6,828,159 B1, 1999.
(30) Kolmakov, K.; Belov, V. N.; Wurm, C. A.; Harke, B.; Leutenegger, M.; Eggeling, C.; Hell, S. W. A Versatile Route to Red-Emitting Carbopyronine Dyes for Optical Microscopy and Nanoscopy. *Eur. J. Org. Chem.* **2010**, *19*, 3593−3610.
(31) Butkevich, A. N.; Mitronova, G. Y.; Sidenstein, S. C.; Klocke, J. L.; Kamin, D.; Meineke, D. N. H.; D'Este, E.; Kraemer, P.-T.; Danzl, J. G.; Belov, V. N.; Hell, S. W. Fluorescent Rhodamines and Fluorogenic Carbopyronines for Super-Resolution STED Microscopy in Living Cells. *Angew. Chem., Int. Ed.* **2016**, *55*, 3290−3294.
(32) Bachman, J. L.; Pavlich, C. I.; Boley, A. J.; Marcotte, E. M.; Anslyn, E. V. Synthesis of Carboxy ATTO 647N Using Redox Cycling for Xanthone Access. *Org. Lett.* **2020**, *22*, 381−385.
(33) Grimm, J. B.; Klein, T.; Kopek, B. G.; Shtengel, G.; Hess, H. F.; Sauer, M.; Lavis, L. D. Synthesis of a Far-Red Photoactivatable Silicon-Containing Rhodamine for Super-Resolution Microscopy. *Angew. Chem., Int. Ed.* **2016**, *55*, 1723−1727.
(34) Chai, X.; Cui, X.; Wang, B.; Yang, F.; Cai, Y.; Wu, Q.; Wang, T. Near-Infrared Phosphorus-Substituted Rhodamine with Emission Wavelength above 700 nm for Bioimaging. *Chem.—Eur. J.* **2015**, *21*, 16754−16758.
(35) Butkevich, A. N.; Belov, V. N.; Kolmakov, K.; Sokolov, V. V.; Shojaei, H.; Sidenstein, S. C.; Kamin, D.; Matthias, J.; Vlijm, R.; Engelhardt, J.; Hell, S. W. Hydroxylated Fluorescent Dyes for Live-Cell Labeling: Synthesis, Spectra and Super-Resolution STED Microscopy. *Chem.—Eur. J.* **2017**, *23*, 12114−12119.
(36) Butkevich, A. N.; Lukinavičius, G.; D'Este, E.; Hell, S. W. Cell-Permeant Large Stokes Shift Dyes for Transfection-Free Multicolor Nanoscopy. *J. Am. Chem. Soc.* **2017**, *139*, 12378−12381.
(37) Koide, Y.; Urano, Y.; Hanaoka, K.; Terai, T.; Nagano, T. Evolution of Group 14 Rhodamines as Platforms for Near-Infrared Fluorescence Probes Utilizing Photoinduced Electron Transfer. *ACS Chem. Biol.* **2011**, *6*, 600−608.
(38) Beija, M.; Afonso, C. A. M.; Martinho, J. M. G. Synthesis and Applications of Rhodamine Derivatives as Fluorescent Probes. *Chem. Soc. Rev.* **2009**, *38*, 2410−2433.
(39) Jablonski, J. Self-Depolarization and Decay of Photo-luminescence of Solutions. *Acta Phys. Pol.* **1955**, *14*, 295−307.
(40) Lakowicz, J. R.; Malicka, J.; D'Auria, S.; Gryczynski, I. Release of the Self-Quenching of Fluorescence Near Silver Metallic Surfaces. *Anal. Biochem.* **2003**, *320*, 13−20.
(41) Rich, R. M.; Mummert, M.; Foldes-Papp, Z.; Gryczynski, Z.; Borejdo, J.; Gryczynski, I.; Fudala, R. Detection of Hyaluronidase Activity Using Fluorescein Labeled Hyaluronic Acid and Fluorescence Correlation Spectroscopy. *J. Photochem. Photobiol., B* **2012**, *116*, 7−12.
(42) López Arbeloa, I.; Ruiz Ojeda, P. Dimeric States of Rhodamine B. *Chem. Phys. Lett.* **1982**, *87*, 556−560.
(43) Arbeloa, F. L.; Ojeda, P. R.; Arbeloa, I. L. Flourescence Self-quenching of the Molecular Forms of Rhodamine B in Aqueous and Ethanolic solutions. *J. Lumin.* **1989**, *44*, 105−112.
(44) Valdes-Aguilera, O.; Neckers, D. C. Aggregation Phenomena in Xanthene dyes. *Acc. Chem. Res.* **1989**, *22*, 171−177.
(45) Notably, substitution of the rhodamine core with sulfonate groups has been shown to diminish self-quenching by inhibiting fluorophore dimerization, see Panchuk-Voloshina, N.; Haugland, R. P.; Bishop-Stewart, J.; Bhalgat, M. K.; Millard, P. J.; Mao, F.; Leung, W.-Y.; Haugland, R. P. Alexa Dyes, a Series of New Fluorescent Dyes

https://doi.org/10.1021/acs.bioconjchem.2c00103
Bioconjugate Chem. XXXX, XXX, XXX−XXX

That Yield Exceptionally Bright, Photostable Conjugates. *J. Histochem. Cytochem.* **1999**, *47*, 1179−1188.
(46) Luchowski, R.; Matveeva, E.; Gryczynski, I.; Terpetschnig, E.; Patsenker, L.; Laczko, G.; Borejdo, J.; Gryczynski, Z. Single Molecule Studies of Multiple-fluorophore Labeled Antibodies. Effect of Homo-FRET on the Number of Photons Available Before Photobleaching. *Curr. Pharmacogenomics* **2008**, *9*, 411−420.
(47) Szabó, Á.; Szendi-Szatmári, T.; Ujlaky-Nagy, L.; Rádi, I.; Vereb, G.; Szöllősi, J.; Nagy, P. The Effect of Fluorophore Conjugation on Antibody Affinity and the Photophysical Properties of Dyes. *Biophys. J.* **2018**, *114*, 688−700.
(48) Lakowicz, J. R.; Geddes, C. D.; Gryczynski, I.; Malicka, J.; Gryczynski, Z.; Aslan, K.; Lukomska, J.; Matveeva, E.; Zhang, J.; Badugu, R.; Huang, J. Advances in Surface-Enhanced Fluorescence. *J. Fluoresc.* **2004**, *14*, 425−441.
(49) Knox, R. S. Theory of Polarization Quenching by Excitation Transfer. *Physica* **1968**, *39*, 361−386.
(50) Fudala, R.; Mummert, M. E.; Gryczynski, Z.; Rich, R.; Borejdo, J.; Gryczynski, I. Lifetime-Based Sensing of the Hyaluronidase Using Fluorescein Labeled Hyaluronic Acid. *J. Photochem. Photobiol., B* **2012**, *106*, 69−73.
(51) Conroy, E. M.; Li, J. J.; Kim, H.; Algar, W. R. Self-Quenching, Dimerization, and Homo-FRET in Hetero-FRET Assemblies with Quantum Dot Donors and Multiple Dye Acceptors. *J. Phys. Chem. C* **2016**, *120*, 17817−17828.
(52) Lu, Y.; Penzkofer, A. Absorption Behavior of Methanolic Rhodamine 6G Solutions at High Concentration. *Chem. Phys.* **1986**, *107*, 175−184.
(53) Bojarski, P.; Kulak, L.; Bojarski, C.; Kawski, A. Nonradiative Excitation Energy Transport in One-Component Disordered Systems. *J. Fluoresc.* **1995**, *5*, 307−319.
(54) Aggregation of fluorophores of the same identity has little or no dependence upon the photophysical properties of the probes, but FRET between two identical fluorophores does require that fluorophores possess small stokes shifts, a common characteristic of xanthene-based dyes. The short shift in emission relative to excitation wavelengths results in significant overlap of these spectra and the ability to transfer energy through nonradiative processes. See refs 49 and 50 for more detail.
(55) Swaminathan, J.; Boulgakov, A. A.; Hernandez, E. T.; Bardo, A. M.; Bachman, J. L.; Marotta, J.; Johnson, A. M.; Anslyn, E. V.; Marcotte, E. M. Highly Parallel Single-Molecule Identification of Proteins in Zeptomole-Scale Mixtures. *Nat. Biotechnol.* **2018**, *36*, 1076−1082.
(56) Alfaro, J. A.; Bohländer, P.; Dai, M.; Filius, M.; Howard, C. J.; van Kooten, X. F.; Ohayon, S.; Pomorski, A.; Schmid, S.; Aksimentiev, A.; Anslyn, E. V.; Bedran, G.; Cao, C.; Chinappi, M.; Coyaud, E.; Dekker, C.; Dittmar, G.; Drachman, N.; Eelkema, R.; Goodlett, D.; Hentz, S.; Kalathiya, U.; Kelleher, N. L.; Kelleher, N. L.; Kelly, R. T.; Kelman, Z.; Kim, S. H.; Kuster, B.; Rodriguez-Larrea, D.; Lindsay, S.; Maglia, G.; Marcotte, E. M.; Marino, J. P.; Masselon, C.; Mayer, M.; Samaras, P.; Sarthak, K.; Sepiashvili, L.; Stein, D.; Wanunu, M.; Wilhelm, M.; Yin, P.; Meller, A.; Joo, C. The Emerging Landscape of Single-molecule Protein Sequencing Technologies. *Nat. Methods* **2021**, *18*, 604−617.
(57) Fish, K. N. Total Internal Reflection Fluorescence (TIRF) Microscopy. *Curr. Protoc. Cytom.* **2009**, *10*, 2A.2.1.
(58) Edman, P.; Begg, G. A Protein Sequenator. *Eur. J. Biochem.* **1967**, *1*, 80−91.
(59) The amino acid residue is identified by the chemical modification strategy used to attach the fluorophore. A representative example can be seen here Hernandez, E. T.; Swaminathan, J.; Marcotte, E. M.; Anslyn, E. V. Solution-phase and Solid-phase Sequential, Selective Modifcation of Side Chains in KDYWEC and KDYWE as Models for Usage in Single-molecule Protein Sequencing. *New J. Chem.* **2017**, *41*, 462−469.
(60) Edman degradation requires treatment of the surface-bound peptides with phenyl isothiocyanate (PITC) and pyridine, and separately, neat trifluoroacetic acid (TFA). Both conditions require 40 °C and several hours of incubation per treatment.
(61) To identify fluorophores ideal for fluorosequencing, a broad range of different fluorescent probes were evaluated prior to this study. Fluorophores were attached to solid supported TentaGel resins and incubated for over 20 h with either PITC and pyridine or TFA. The fluorescence output of the beads was evaluated before and after treatment to identify fluorophores that could be used for this strategy. See ref 55 Supporting Information for additional details.
(62) While we hoped to explore peptides bearing multiple fluorophores of different identity (e.g. both 2 and 3 on different residues as in ref 21), this required quite significant synthetic effort for orthogonal labeling in the context of the long-linker strategy. Effort was instead focused on multiple fluorophores of the same identity for ease of synthetic manipulation.
(63) Viger, M. L.; Live, L. S.; Therrien, O. D.; Boudreau, D. Reduction of Self-Quenching in Fluorescent Silica-Coated Silver Nanoparticles. *Plasmonics* **2008**, *3*, 33−40.
(64) Zhang, J.; Fu, Y.; Chowdhury, M. H.; Lakowicz, J. R. Single-Molecule Studies on Fluorescently Labeled Silver Particles: Effects of Particle Size. *J. Phys. Chem. C* **2008**, *112*, 18−26.
(65) Bardhan, R.; Grady, N. K.; Cole, J. R.; Joshi, A.; Halas, N. J. Fluorescence Enhancement by Au Nanostructures: Nanoshells and Nanorods. *ACS Nano* **2009**, *3*, 744−752.
(66) Golberg, K.; Elbaz, A.; Zhang, Y.; Dragan, A. I.; Marks, R.; Geddes, C. D. Mixed-Metal Substrates for Applications in Metal-Enhanced Fluorescence. *J. Mater. Chem.* **2011**, *21*, 6179−6185.
(67) For examples of common fluorophore linkers see: Schepers, B.; Gohlke, H. AMBER-DYES in AMBER: Implementation of Fluorophore and Linker Parameters into AmberTools. *J. Chem. Phys.* **2020**, *152*, 221103. And Marek, M.; Kaiser, K.; Gruber, H. J. Biotin−Pyrene Conjugates with Poly(ethylene glycol) Spacers Are Convenient Fluorescent Probes for Avidin and Streptavidin. *Bioconjugate Chem.* **1997**, *8*, 560−566.
(68) Hoch, D. G.; Abegg, D.; Adibekian, A. Cysteine-reactive Probes and Their use in Chemical Proteomics. *Chem. Commun.* **2018**, *54*, 4501−4512.
(69) Despite that fluorophores **2** and **3** were the most robust fluorophores identified for fluorosequencing, photobleaching as well as loss of fluorescence still occur with longer times subjected to Edman degradation chemistry as well as fluorescent excitation.
(70) The propargylamide click handle **12** is analogous to those generated in ubiquitin tags, see: Ekkebus, R.; van Kasteren, S. I.; Kulathu, Y.; Scholten, A.; Berlin, I.; Geurink, P. P.; de Jong, A.; Goerdayal, S.; Neefjes, J.; Heck, A. J. R.; Komander, D.; Ovaa, H. On Terminal Alkynes That Can React with Active-Site Cysteine Nucleophiles in Proteases. *J. Am. Chem. Soc.* **2013**, *135*, 2867−2870.
(71) While the förster radius of the fluorophores homo-FRET interactions could likely still occur with $(PEG)_{10}$ (<100 Å), even longer heterofunctionalized spacers were not readily available at the time of this study. We anticipated that this spacing would still provide an ample difference relative to the shorter linkers inherent with the fluorophores.
(72) The CuAAC installation strategy was selected due to the ease of preparation of the peptides relative to the commercial cost of the specialized fluorophores. We initially envisioned functionalizing the fluorophores with iodoacetamide handles directly, however, due to the cost of minute quantities of fluorophores and the additional synthetic manipulations required, that strategy was not pursued.
(73) Acetylation was performed to inhibit photo-induced electron transfer (PET) quenching from the free lonepairs of terminal nitrogen atoms with the appended fluorophores.
(74) Attempts to separate the constitutional isomers by chromatography were unsuccessful. This was further the case with all single-fluorophore labelled peptides (**14**, **16**, **20**, **22**).
(75) While the click reaction was initially attempted using the Boc protecting group on the terminal amine, as was in the case of the short-linker peptides, no desired reaction was observed with this set of conditions. It appeared that some amount of peptide was being

https://doi.org/10.1021/acs.bioconjchem.2c00103
Bioconjugate Chem. XXXX, XXX, XXX−XXX

deprotected during the reaction, leading to free amine that likely coordinated to copper. As such, switching to the Fmoc protecting group was performed. Although, this was further met with minor challenges as well, see the Supporting Information for more detail.
(76) FLT for Atto peptides was calculated based on fitting to a single-exponential decay function. FLT for TMR peptides is reported as the intensity weighted average lifetime following fit to a double-exponential decay. Additional information on FLT can be found in the Solution phase Fluorescence Analysis section of the SI.
(77) Swaminathan, J.; Boulgakov, A. A.; Marcotte, E. M. A Theoretical Justification for Single Molecule Peptide Sequencing. *PLoS Comput. Biol.* **2015**, *11*, No. e1004080.
(78) Mutch, S. A.; Fujimoto, B. S.; Kuyper, C. L.; Kuo, J. S.; Bajjalieh, S. M.; Chiu, D. T. Deconvolving Single-Molecule Intensity Distributions for Quantitative Microscopy Measurements. *Biophys. J.* **2007**, *92*, 2926−2943.
(79) Hanley, D. C.; Harris, J. M. Quantitative Dosing of Surfaces with Fluorescent Molecules: Characterization of Fractional Monolayer Coverages by Counting Single Molecules. *Anal. Chem.* **2001**, *73*, 5030−5037.
(80) Coffman, V. C.; Wu, J.-Q. Counting Protein Molecules Using Quantitative Fluorescence Microscopy. *Trends Biochem. Sci.* **2012**, *37*, 499−506.
(81) Gordon, M. P.; Ha, T.; Selvin, P. R. Single-molecule High-resolution Imaging with Photobleaching. *Proc. Natl. Acad. Sci. U.S.A.* **2004**, *101*, 6462−6465.

https://doi.org/10.1021/acs.bioconjchem.2c00103
Bioconjugate Chem. XXXX, XXX, XXX−XXX